Biomedical Signal Processing and Control 5 (2010) 21–31

Contents lists available at ScienceDirect

Biomedical Signal Processing and Control

journal homepage: www.elsevier.com/locate/bspc

Discrimination between ischemic and artifactual ST segment events in Holter recordings

Ana Mincholé [a,b,*], Franc Jager [c], Pablo Laguna [b,a]

[a] Centro de Investigación Biomédica en Red (CIBER-BBN), Spain
[b] Communications Technology Group (GTC) at the Aragón Institute of Engineering Research (I3A), University of Zaragoza, María de Luna 1, 50018 Zaragoza, Spain
[c] Faculty of Computer and Information Science, University of Ljubljana, Ljubljana, Slovenia

ARTICLE INFO

Article history:
Received 10 February 2009
Received in revised form 3 September 2009
Accepted 7 September 2009
Available online 12 November 2009

Keywords:
Ischemia detection
Classification analysis
ECG processing
Holter recordings

ABSTRACT

ST segment changes provide a sensitive marker in the diagnosis of myocardial ischemia in Holter recordings. However, not only do the mechanisms of ischemia result in ST segment deviation, but also heart rate related episodes, body position changes or conduction changes among others, which are considered artifactual events when ischemia is the target. In order to distinguish between them, the very similar signatures of ST modifications has led us to look for other ECG indices such as heart rate-based indices, correlation between the absolute ST segment deviation and heart rate series, the interval between the T_{apex} and the T_{end}, T wave amplitude, the signal-to-noise ratio and changes in the upward/downward slopes of the QRS complex. A discrimination analysis between the three types of events: ischemia, heart rate related episodes and sudden step ST changes (body position changes and conduction changes) has been performed on the Long-Term ST Database, reaching an accuracy of 82.3%. If we focus on distinguishing between different ST signatures, transient episodes (ischemic and heart rate related) and sudden step ST changes, it results in a sensitivity of 76.8% and a specificity of 98.3%. When classifying ischemia from heart rate related episodes, both with a very similar ST level pattern, a sensitivity of 84.5% and a specificity of 86.6% are reached. Finally, for separating ischemia from any other ST event, a sensitivity of 74.2% and a specificity of 93.2% are obtained.

1. Introduction

Myocardial ischemia is the most common cause of death in industrialized countries and, as a consequence, its early diagnosis and treatment is of great importance. It can be defined as the imbalance between oxygen/nutrient delivery with regard to myocardial requirements. "Supply ischemia" results from a partial occlusion of a coronary artery, reducing the amount of oxygenated blood to the myocardium. The term "demand ischemia" refers to a condition where an increased oxygen demand caused by exercise, tachycardia or emotion, leads to a transitory imbalance [1,2].

Ischemia is commonly a transient phenomena, which is time constrained, and could be missed during physical examination and routine electrocardiography (ECG) because these procedures permit only a few seconds of observation. To diagnose ischemia, longer periods of ECG recording are required while the patient is pursuing his or her normal routine. Holter monitoring gives a constant reading of two to three channels of ECG data over a 24-h period.

The cellular modifications generated by acute ischemia are responsible for changes in the ST segment, which make ST segment changes an early marker of ischemia [3]. Electrocardiographic images of ischemia are different depending on whether the ischemic area affects mainly the sub-endocardium or the sub-epicardium. In the case of sub-endocardial ischemia, ST depression appears at different intensities according to its degree while in the case of sub-epicardial, also called transmural ischemia, ST elevation occurs [3].

Several techniques that automate ischemia detection have been proposed during the last decade and mostly rely on ST changes [4,5]. However, in addition to ischemic ST episodes (*IE*), there are other ST events such as heart rate related episodes (*HRE*), body position changes (*BPCE*) or conduction changes (*CCE*) which also result in ST segment modifications being considered artifactual events when ischemia is the target. This makes ischemia detection in ambulatory recordings a difficult task.

As mentioned above, ischemia could originate as supply or demand ischemia. In the database we are using, the Long-Term ST Database (LTST DB) [6], ischemia is not classified as demand or supply. An ST event is annotated as *IE* when it is associated with a

* Corresponding author at: Communications Technology Group (GTC) at the Department of Electronic Eng. and Communications, University of Zaragoza, María de Luna 1, 50018 Zaragoza, Spain.
E-mail address: minchole@unizar.es (A. Mincholé).

1746-8094/$ – see front matter © 2009 Elsevier Ltd. All rights reserved.
doi:10.1016/j.bspc.2009.09.001

patient with a clinical history showing evidences of cardiac pathology. On the other hand, if there is an episode associated with an increase or alteration of heart rate in the ECG and other clinical investigations do not suggest ischemia, these episodes are annotated as *HRE*. Typically, the ST level is measured at the point J + 80 ms, or at the point J + 60 ms if the heart rate exceeds 120 bpm [6]. This adaptation of the ST level to heart rate is still a crude adaptation so it produces ST segment episodes with a similar signature to ischemic episodes generated by the T wave incursion into the point where the ST level is measured. These ST events, that are not associated to ischemia mechanisms, are denoted as *HRE*.

The dynamics of the different ST events is different in each case. *HRE* as well as *IE* are considered transient ST segment episodes (*TE*) and characterized by a length and an extremum deviation. In contrast, *BPCE* and *CCE*, characterized with a sudden shift in the ST level function, are denoted as sudden step events (SSE) and are characterized by the time instance they occur.

The novelty of the present work lies in the use of several indices based on repolarization and depolarization intervals to distinguish in Holter recordings between different events scenarios called tasks:

Task 1 Distinguishing between the three independent and different origin types of ST events: the target *IE*, the artifactual *HRE* and the also artifactual *SSE*.
Task 2 Distinguishing between the different ST level signatures: transient (*TE*) and sudden step ST change (*SSE*).
Task 3 Distinguishing between *IE* and *HRE*, both with a very similar ST level pattern, so being the more problematic to differentiate by automatic ischemia detectors.
Task 4 Distinguishing between *IE* and non-ischemic events (*NIE*) in order to isolate the ischemic problem.

The availability of the annotated LTST DB has provided the possibility of quantifying the results of classifiers such as those presented in this work, always under the framework in which the annotations were developed.

Previous studies have covered some of the proposals outlined in this article. Task 3, distinguishing between *IE* and *HRE*, has not been the subject of much analysis due to the fact that no other database provides annotations of *HRE*. The only study is [7] and this also uses the LTST DB. In the work in [7], the selected features for classification were changes of heart rate, changes of time domain morphologic parameters of the ST segment and changes of the Legendre orthonormal polynomial coefficients of the ST segment, all obtained at 20 s intervals at the beginning and at the extrema of each ST episode, and achieving a sensitivity when classifying ischemia and heart rate related episodes of 77.9% and a specificity of 73.9%.

Similarly to Task 4, the 2003 Physionet/Computers in Cardiology Challenge [8] consisted of classifying ST changes as ischemic (*IE*) or non-ischemic (*HRE*, *BPCE* or *CCE*) using a set of 43 freely available annotated records of the LTST DB as a training set and the remaining 43 as a test set. Note that not all annotated ST change events from the database were used, but only the selected subset. The top scoring entry of this challenge [9] achieved a performance in terms of sensitivity/positive predictivity of 98%/83% considering only the change in ST level relative to the baseline ST level, provided by the database and manually corrected by experts, and based on level thresholding within specified time windows.

To separate detection from classification problems, we assume the episodes are correctly detected so we take the manual annotations (onset, extremum and offset) provided with the database as the detection output and just focus on the classification problem. Automatic detection rules can be found in works by García et al. [4] and Smrdel and Jager[5].

2. Materials and methods

2.1. The data: Long-Term ST Database

The LTST DB [6] contains 86 24-h duration ambulatory ECG records of 80 patients sampled at $f_s = 250$ Hz. This database offers a very accurate representation of "clinical world" data with two- or three-lead records with a great variety of lead combinations. Each two-channel record contains one of the following pairs: one of the bipolar leads recorded at precordial positions, denoted as pseudo V2–V5, together with modified limb lead III (MLIII); or pseudo-lead V5 and pseudo-lead V2; or modified limb lead L2 (ML2) and modified lead V2 (MV2). The leads used in the three-channel records included: a combination from leads pseudo V3–V6, II and aVF, or Zymed's EASI lead system [10] with the leads E-S, A-S and A-I.

Complete expert annotations have been provided for the database following three different annotation protocols. Electrocardiogram waveform is not enough to diagnose myocardial ischemia, so the gold standard for annotating a transient ST segment, *IE* or *HRE*, was based not only on ECG waveforms but also on detailed clinical information from the subjects including other clinical investigations, the clinical history and the opinion of expert annotators of the database [6]. Thus, a classification of a particular episode can be driven by a previous knowledge about the patient rather than physiological evidences. This is one limitation we should have in mind when analysing the results.

Annotations include *IE* and other ST segment events such as *HRE*, *BPCE* and *CCE*, providing an extensive tool to evaluate classifiers aimed at distinguishing among ST episodes of different origin.

One transient ST episode (*TE*) has to be significant to be annotated according to the following rules: (a) an episode beginning when the magnitude of the ST deviation first exceeds 50 μV, (b) the deviation must reach a magnitude of $V_{\min}$ or more throughout a continuous interval of at least $T_{\min}$ s and (c) an episode ending when the deviation becomes smaller than 50 μV, provided that it does not exceed 50 μV in the following 30 s.

Three different protocols A, B and C are set depending on $V_{\min}$ and $T_{\min}$:

- Protocol A: $V_{\min} = 75$ μV and $T_{\min} = 30$ s.
- Protocol B: $V_{\min} = 100$ μV and $T_{\min} = 30$ s.
- Protocol C: $V_{\min} = 100$ μV and $T_{\min} = 60$ s.

Hereinafter we will denote the "ischemia group" as *IG*, the "heart rate related group" as *HRG* and the "sudden step group", comprising *BPCE* and *CCE*, as *SSG*. *TG* will stand for the transient group composed of *IG* and *HRG*, and *NIG* will stand for the non-ischemic group that comprises *HRE*, *BPCE* and *CCE*. A comprehensive scheme is shown in Table 1(a).

The classification evaluation of this work has been done for the three different sets relative to the annotation protocols. The number of episodes of each type used for the classification analysis in protocols A, B and C is shown in Table 1(b). The number of analysed events is slightly lower than in the original database [6] (in square brackets in Table 1(b)) due to the fact that some episodes at the beginning of the record have not got any onset annotations since their onsets start before the beginning of the records and were excluded from the analysis.

When classifying *IG* and *HRG*, we have added T wave related variables which have caused us to additionally remove manually those episodes with unreliable annotations in the T wave delineation process, resulting in the number of episodes for protocols A, B and C as presented in parentheses in Table 1(b).

Any significant sudden step change of the ST level function accompanied by a simultaneous sudden step change in QRS

Table 1
(a) Summary of ST events grouping and their acronyms. (b) Number of *IE*, *HRE* and *SSE* used in discrimination for each annotation protocol. These numbers are a bit lower than in the original database (see text) that are displayed in square brackets. The numbers in parentheses refer to episodes that additionally allow reliable T wave delineation when these parameters are to be used.

(a) Types of ST episodes

ST events		
Non-Ischemic group (NIG)	*Ischemic group* (IG)	Transient group (TG)
	Heart rate related group (HRG)	
	Axis Shifts	Sudden step group (SSG)
	Conduction changes	

(b) Number of episodes used for classification

	Protocol A			Protocol B			Protocol C		
IG	[1795]	1788	(*1163*)	[1130]	1126	(*623*)	[857]	855	(*505*)
HRG	[516]	513	(*358*)	[234]	232	(*112*)	[116]	115	(*54*)
SSG		2388			2388			2388	
Total		4689	(*1521*)		3746	(*735*)		3358	(*559*)

complex morphology was annotated as significant *BPCE* or significant *CCE*, according to its nature (see Fig. 1).

Annotations are attached to the lead or leads where the episode is significant, so all the study has been done considering the lead to which the annotated episodes are linked. An example of ST traces in the four different cases can be found in Fig. 1.

2.2. ECG preprocessing and beat identification

Before deriving index series from the ECG, typical preprocessing techniques are applied on the raw ECG signal, $x_l(n)$, where l is the corresponding lead and n is the sample index. This preprocessing stage consists of first applying a QRS detector [11] in order to find QRS fiducial points of each ith beat (θ_i) and selecting only normal beats classified according to [11], then baseline wander attenuation using cubic splines is performed [12] and finally those beats with differences in mean isoelectric level with respect to adjacent beats larger than 400 μV are rejected. There are different factors such as motion artifacts that distort the ECG signal so an extra beat rejection rule is applied for those whose signal-to-noise ratio (SNR), estimated as the peak-to-peak QRS amplitude over the RMS value of the high-frequency noise (above 25 Hz), differs more than 20 dB from the running exponentially averaged SNR series. The forgetting factor of the exponential averaging is set to 0.02 as in [13].

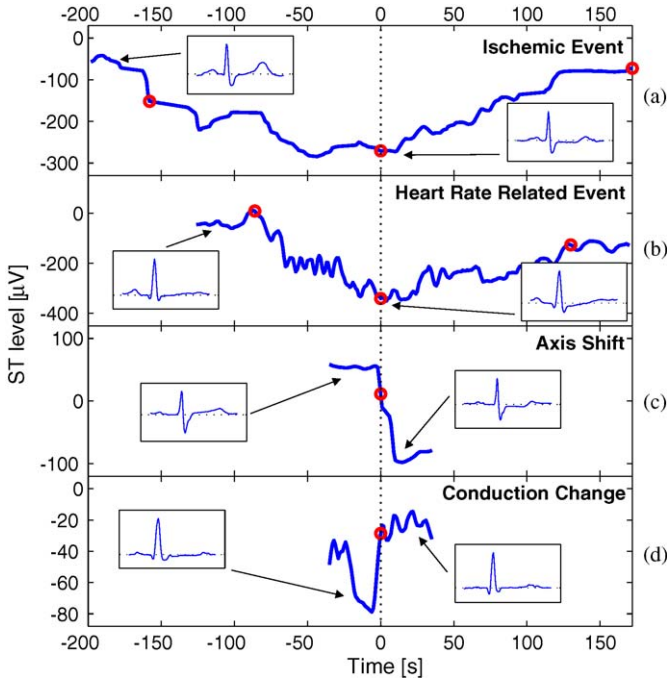

Fig. 1. Example of the ST segment deviation caused by the four different annotated episodes: (a) ischemic, (b) heart rate related, (c) axis shifts and (d) conduction change events. The circles indicate the annotated onset, extremum and offset in transient episodes and the occurrence time in the sudden step changes. Time "0" is referred to the extremum in *TE*, or occurrence time in *SSE*.

2.3. Indices for the discriminant analysis

In this work, different ECG features $(\mathcal{I})$ and their transient variations $(\Delta\mathcal{I})$, measured from repolarization, depolarization and heart rate indices have been used in the discriminant analysis.

In order to distinguish between both transient episodes, *IG* and *HRG*, these features have been computed over three different intervals (I_1, I_2 and I_3) of 20 s duration each (the duration was selected empirically), located as described in Fig. 2(a). I_1 is defined as 20 s interval ending at the sample where the episode begins, I_2 as 20 s interval starting at the sample of the episode onset and I_3 as 20 s interval centered at the extremum episode sample. The changes of the mean feature value in interval I_k with respect to I_j $(\Delta\mathcal{I}_{jk})$ have been computed and proposed as indices for the classification analysis (see Eq. (1)):

$$\Delta\mathcal{I}_{jk} = \frac{\sum_{i\in I_k}\mathcal{I}(i)}{N_{I_k}} - \frac{\sum_{i\in I_j}\mathcal{I}(i)}{N_{I_j}} \qquad j,k = 1,2,3 \quad \text{and} \quad j \neq k \qquad (1)$$

where i is an integer denoting the ith beat order in interval I and N_{I_k} and N_{I_j} are the number of beats contained in interval I_k and I_j respectively.

Alternatively, when discriminating between the three types of events including *IG*, *HRG* and *SSG*, only two intervals are considered since *SSG* is characterized by a unique mark. For *SSG* two intervals of 20 s each is defined; I_1, just before the event and I_2, just after, which is going to be paired to the I_3 interval of the *TG* group (*IG* plus

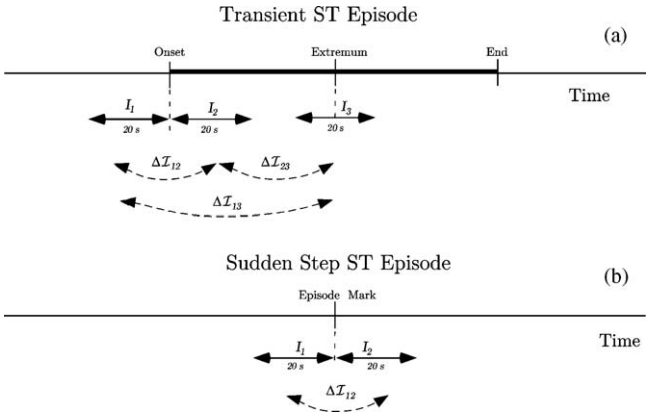

Fig. 2. (a) For discriminating between transient events, the three different intervals I_1, I_2 and I_3 used to compute $\Delta\mathcal{I}_{12}$, $\Delta\mathcal{I}_{13}$ and $\Delta\mathcal{I}_{23}$ are shown. (b) For sudden step events, only two intervals I_1 and I_2, are defined.

HRG) when the two ST signatures are to be discriminated (see Fig. 2(b)).

All the indices are computed over the ECG after the preprocessing stage. Some of them are shown in Fig. 3(a).

2.3.1. Repolarization indices

- As has been previously described, the ST level is a common marker of ischemia and has therefore been included in the classification analysis. The underlying mechanism responsible of the shift in the ST level is that ischemic tissue produces an injury current [3]. It has been found that the angular difference in the non-ischemic and ischemic case is very consistent over the entire ST and T wave segment, and in some cases the terminal portion of the QRS complex. The ST level series is estimated at each *i*th beat and lead by averaging 8 ms (to make the measurement more stable) of the preprocessed ECG signal starting from a heart rate related sample reference ($n^i_{\mathrm{ST}_0}$) [14]:

$$n^i_{\mathrm{ST}_0} = \theta_i + \frac{40}{1000} f_s + 1.3\sqrt{\frac{rr_i}{1000} f_s} \tag{2}$$

where θ_i represents the sample of the QRS fiducial point defined as the center of gravity of the QRS complex and $rr_i = \theta_i - \theta_{i-1}$ the RR interval at the *i*th beat in sample units.

Changes in the deviation of the ST level are denoted as $\Delta\mathcal{I}_{\mathrm{ST}_{12}}$, $\Delta\mathcal{I}_{\mathrm{ST}_{13}}$ and $\Delta\mathcal{I}_{\mathrm{ST}_{23}}$. The absolute values of these changes in the ST level series are also considered for the classification analysis and denoted as $|\Delta\mathcal{I}_{\mathrm{ST}_{12}}|$, $|\Delta\mathcal{I}_{\mathrm{ST}_{13}}|$ and $|\Delta\mathcal{I}_{\mathrm{ST}_{23}}|$.

- The root mean square (RMS) of the difference of the ST segment with respect to the ST of a reference beat ($\mathcal{I}_{\mathrm{RMS}}$) is analysed. The hypothesis here is that differences in the area under the ST segment is a more robust measurement than the ST level itself, since it includes information about changes in energy of this segment [4].

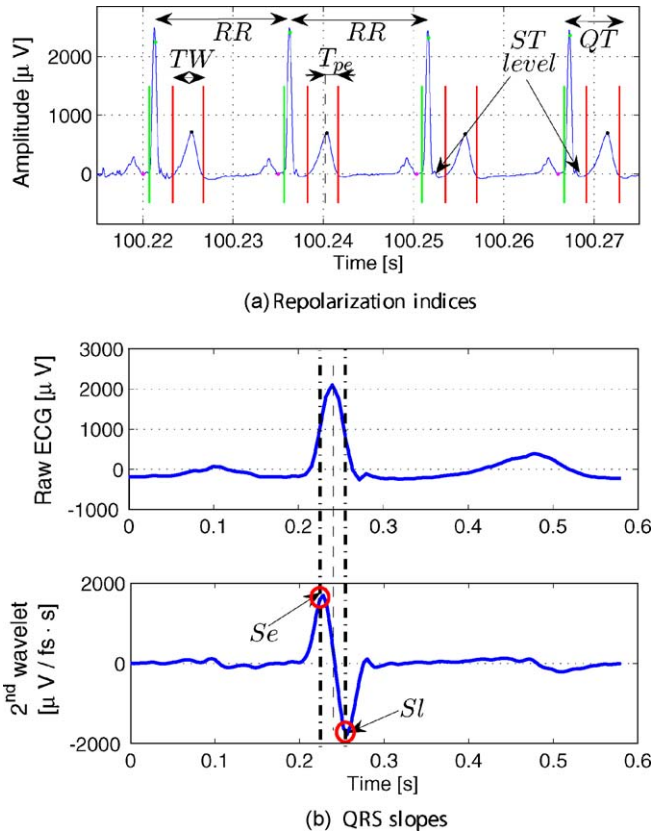

Fig. 3. (a) The different intervals used for obtaining the series of T width (T_w), T_{apex} to T_{end} interval (T_{pe}), QT interval (QT) and the RR interval measured to compute the heart rate series (HR) are shown. The ST level series is calculated by averaging the first 8 ms of the ST segment. (b) In the upper figure, the QRS complex of the raw ECG signal and, in the lower figure, its second scale wavelet transform are shown. The maximum and minimum of the wavelet transform correspond to the two steepest slopes. Note that zero crossing of the wavelet transform corresponds with the peak of the QRS complex.

- The root mean square (RMS) of the difference of the ST segment with respect to the ST of a reference beat ($\mathcal{I}_{\mathrm{RMS}}$) is analysed. The hypothesis here is that differences in the area under the ST segment is a more robust measurement than the ST level itself, since it includes information about changes in energy of this segment [4].

In order to avoid the influence of high-frequency noise in the calculation of the RMS difference series, the preprocessed ECG signal is further low-pass filtered using a linear phase FIR filter with a cutoff frequency of 25 Hz at the ST segment.

The ST segmentation is performed by selecting a fixed length window of 50 ms from the heart rate related sample reference $n^i_{\mathrm{ST}_0}$. The segmented ST window signal $x^i_{\mathrm{ST},l}(n)$ is defined as:

$$x^i_{\mathrm{ST},l}(n) = x_l(n^i_{\mathrm{ST}_0} + n) \qquad n = 0, \ldots, N-1 \tag{3}$$

where $N = (50/1000) f_s$ and l is the corresponding lead.

In order to calculate the $\mathcal{I}_{\mathrm{RMS}}$ difference series, a reference beat, $\bar{x}_{\mathrm{ST},l}(n)$, has to be defined. We create an ST series defined as the first sample of the ST segment of each beat, $x^i_{\mathrm{ST},l}(1)$ with $i = 1, \ldots, M$ where M is the number of beats in the record. In this series, an interval of 30 min called the "*basal interval*" is searched with two restrictions: having the shortest peak-to-peak amplitude in the series and the whole interval series being below 4/3 of the $x^i_{\mathrm{ST},l}(1)$ absolute median value of the recording. Within this "*basal interval*" 100 beats are averaged to calculate the reference beat in each lead $\bar{x}_{\mathrm{ST},l}(n)$.

Finally, a first RMS difference series, $y_l(\theta_i)$ is calculated using the following equation:

$$y_l(\theta_i) = \sqrt{\frac{1}{N}\sum_{n=0}^{N-1}\left(x^i_{\mathrm{ST},l}(n) - \bar{x}_{\mathrm{ST},l}(n)\right)^2} \tag{4}$$

where l is the corresponding lead.

As an outlier rejection, a median filter of 5 beats length is subsequently used on the $y_l(\theta_i)$ series. This series is evenly resampled to 1 Hz and an exponential running average (with a forgetting factor set to 0.05) is applied to smooth the series resulting in a RMS-series suitable for analysis and denoted hereinafter by $\mathcal{I}_{\mathrm{RMS}}$.

- The Karhunen–Loéve transform (KLT signature) of the ST–T and QRS complexes are also analysed. Body position changes are often manifested as shifts in the electrical axis and may be misclassified as ischemic changes during ambulatory

monitoring. These shifts in the electrical axis and therefore in the ECG, are manifested as abrupt changes on the QRS and STT complexes, property which can be used to discriminate ischemia from other events.

Previous studies have used the Karhunen–Loéve transform (KLT) to detect non-ischemic episodes such as body position changes or conduction changes [15]. During these non-ischemic events the QRS signatures also change rapidly (generally over a period of half a minute) generating step function features in KLT coefficient series which are useful for discriminating "from just" episodes restricted to repolarization changes. Besides, the KLT of the QRS and ST segment has already been used in differentiating between true ischemic ST segment changes and non-ischemic ST deviations caused by axis shifts [16]. The distance functions used for each complex (QRS and ST–T) at time (θ_i) are simply the distance series between each normalized KLT coefficients vector (in which only the first four components are considered) and a mean reference value (r):

$$\mathcal{I}^e_{\mathrm{KL},l}(\theta_i) = \sqrt{\sum_{j=1}^{4}(\alpha^l_j(\theta_i) - \alpha^l_j(r))^2} \tag{5}$$

with $\alpha^l_j(\theta_i)$ being the jth order KLT coefficient at beat i estimated for the l th lead. The $\alpha^l_j(\theta_i)$ coefficient series is estimated using adaptive filtering to remove noise uncorrelated to the signal, thus improving the KLT estimation [17]. A compromise between noise reduction and convergence time is reached using a step-size parameter for the LMS algorithm of $\mu = 0.10$, that yields a SNR improvement in the series of 10 dB, with a convergence time of one beat [17]. An extra reduction of noise was achieved by applying a median filtering and a smoothing to the KLT trends resulting in the KLT series denoted as: $\mathcal{I}^e_{\mathrm{KL}_{\mathrm{QRS}}}$ and $\mathcal{I}^e_{\mathrm{KL}_{\mathrm{ST-T}}}$. As an alternative, we used the first order Mahalanobis distance functions in order to calculate the KLT series as follows:

$$\mathcal{I}^m_{\mathrm{KL},l}(\theta_i) = \sqrt{\sum_{j=1}^{4}\left(\frac{\alpha^l_j(\theta_i)}{\sigma(\alpha^l_j(\theta_i))}\right)} \tag{6}$$

where $\sigma(\alpha^l_j(\theta_i))$ is the standard deviation of the KLT coefficient series over the beat series.

We applied the same postprocessing procedure as previously explained and obtained the KLT coefficient feature vectors denoted as $\mathcal{I}^m_{\mathrm{KL}_{\mathrm{QRS}}}$ and $\mathcal{I}^m_{\mathrm{KL}_{\mathrm{ST-T}}}$.

- The width of the T wave (T_w) was measured as a potential feature related to repolarization dispersion and eventually related also to ischemia [18], in each lead of the ECG. Delineation was done using a wavelet-based ECG delineator [19]. Changes of the T wave width across the three intervals are denoted as $\Delta\mathcal{I}_{T_w}$.
- Alternatively, changes in the interval from the peak (T_{apex}) to the end (T_{end}) of the T wave (T_{pe}) are measured in each lead. T_{pe} has been proposed as a marker related to transmural dispersion [20] and also as a more robust measurement than T width since it avoids uncertainties in the detection of T onset when ST elevation occurs. These changes measured in each ST episode are denoted as $\Delta\mathcal{I}_{T_{pe}}$.
- The amplitude of the T wave has been taken into account as T wave morphology has been shown as a useful marker of acute transmural ischemic change. It is also a measure of the repolarization dispersion generated by ischemia [21]. Changes in the T wave amplitude ($\Delta\mathcal{I}_{\mathrm{TA}}$), measured referring to the voltage level at the T_{end} fiducial point, have been computed using the delineation marks defined previously.
- QT interval provides information of repolarization dispersion and also is strongly and inversely related to heart rate. The adaptation of the QT interval to the HR has led us to include these changes of QT as a variable for the discrimination between events. Differences in the QT interval have also been measured ($\Delta\mathcal{I}_{\mathrm{QT}}$).
- The correlation between the heart rate series ($\mathcal{I}_{\mathrm{HR}}$) and the $\mathcal{I}_{\mathrm{RMS}}$ of the ST level calculated previously within an interval (I_ρ) of 60 s centered at the onset of the annotated ST episode has also been evaluated as a potential discriminator of *HRG* episodes and referred to as ρ. This has been calculated after resampling the series to an even sampling frequency of 1 Hz in the following way:

$$\rho = \sum_{k\in I_\rho} \frac{(\mathcal{I}_{\mathrm{RMS}}(k) - \mu_{\mathrm{RMS}})(\mathcal{I}_{\mathrm{HR}}(k) - \mu_{\mathrm{HR}})}{N\sigma_{\mathrm{RMS}}\sigma_{\mathrm{HR}}} \tag{7}$$

where μ_{RMS} and μ_{HR} are the mean, and σ_{RMS} and σ_{HR} are the standard deviation of the $\mathcal{I}_{\mathrm{RMS}}$ and $\mathcal{I}_{\mathrm{HR}}$ series respectively in I_ρ, and N the number of samples at the I_ρ interval.

2.3.2. Depolarization indices

Alterations in the late steepest slope of the QRS complex has been proposed as an index to quantify ECG changes in supply ischemia [22]. The conduction velocity reduction generated by ischemia has a strong effect on the downward stroke of the QRS complex, which reduces its amplitude and its slope considerably. Therefore changes in the steepest slopes of the QRS complex referred to as the early (*Se*) and late (*Sl*) slopes are considered in the classification analysis. *Se* and *Sl* can be sequenced either upward/downward or downward/upward depending on the QRS morphology. The QRS slope series are computed from the processing during the QRS delineation [19], using the second scale wavelet transform maximum (minimum) that corresponds to the maximum (minimum) derivative of the QRS complex (see Fig. 3(b)). At the latter stage, the slope series is recomputed by normalizing the QRS amplitude to give the unit mean value at the I_1 interval, so the unit dimension of the slope will be Hz instead of μV/s. Changes in the absolute values of these series (early and late QRS slopes) across the three intervals are taken into account and denoted as $\Delta\mathcal{I}_{\mathrm{Se}}$ and $\Delta\mathcal{I}_{\mathrm{Sl}}$.

2.3.3. Heart rate indices

Changes in the heart rate corresponding to the three intervals are also measured ($\Delta\mathcal{I}_{\mathrm{HR}}$). The absolute value of these changes are also analysed and referred to as $|\Delta\mathcal{I}_{\mathrm{HR}}|$. The mean heart rate values at intervals I_1 and I_3 were computed and denoted as $\mathcal{I}_{\mathrm{HR}_1}$ and $\mathcal{I}_{\mathrm{HR}_3}$ respectively.

2.3.4. Signal-to-noise ratio (SNR) index

With the aim of accounting for the higher noise in *SSG* or *HRG* in comparison with *IG*, the SNR index ($\mathcal{I}_{\mathrm{SNR}}$) has been considered as introduced in Section 2.2.

2.4. Performance evaluation: statistical analysis

First monovariate ANOVA discriminant analysis is performed for each variable so as to establish the individual significance for classification performance. Multivariate discriminant analysis has been used to pick out the ECG indices that best classify different types of episodes. The stepwise approach is then applied, using the Wilk's Lambda minimization as the criteria for inclusion and removal of variables ($F = 3.84$ for inclusion and $F = 2.71$ for rejection) [23]. The classification results are calculated using the cross-validated estimation (leave-one-out). A rule of thumb says that the number of variables used should be lower than the square root of the number of cases of the smallest group of the data set.

Table 2
(a) Summary of the means and standard deviations (mean ± std) of different indices variations used in classification analysis at the annotated ischemic (*IG*), heart rate related (*HRG*) and sudden step ST change (*SSG*) groups applying protocol B, between intervals I_1 and I_3 (in *SSG*, I_3 is replaced by I_2). The *p*-value of each feature is also shown. (b) Summary of the classification performance in terms of the confusion matrix for the annotation protocols A, B and C. The selected set of variables for the prediction are displayed beneath the confusion matrix.

(a) Statistical description of each index

Variables	*IG*	*HRG*	*SSG*	*p*-Value
$\Delta\mathcal{I}_{\mathrm{RMS_{ST}}}$ [μV]	38.7 ± 33.7	24.9 ± 21.3	-0.2 ± 20.1	0
$\Delta\mathcal{I}_{\mathrm{ST}}$ [μV]	-65.0 ± 181.5	-58.8 ± 107.9	-0.4 ± 73.9	$5.1E{-}53$
$\lvert\Delta\mathcal{I}_{\mathrm{ST}}\rvert$ [μV]	152.3 ± 119.0	106.9 ± 60.2	47.7 ± 56.4	$9.8E{-}247$
$\Delta\mathcal{I}_{\mathrm{HR}}$ [bpm]	7.2 ± 15.5	18.9 ± 18.2	1.8 ± 8.6	$2.4E{-}107$
$\lvert\Delta\mathcal{I}_{\mathrm{HR}}\rvert$ [bpm]	12.1 ± 12.0	22.1 ± 14.1	6.5 ± 5.9	$1.4E{-}164$
$\mathcal{I}_{\mathrm{HR_3}}$ [bpm]	90.5 ± 24.1	110.2 ± 21.3	82.6 ± 17.5	$1.4E{-}95$
$\mathcal{I}_{\mathrm{HR_1}}$ [bpm]	83.3 ± 17.9	91.3 ± 15.6	80.8 ± 18.0	$8.1E{-}18$
$\lvert\Delta\mathcal{I}^{e}_{\mathrm{KL_{ST-T}}}\rvert$	0.5 ± 0.6	0.3 ± 0.3	0.1 ± 0.1	$9.7E{-}227$
$\lvert\Delta\mathcal{I}^{m}_{\mathrm{KL_{ST-T}}}\rvert$	1.4 ± 1.4	1.0 ± 0.9	0.2 ± 0.2	$3.7E{-}281$
$\lvert\Delta\mathcal{I}^{e}_{\mathrm{KL_{QRS}}}\rvert$	0.1 ± 0.2	0.1 ± 0.1	0.1 ± 0.1	$2.7E{-}15$
$\lvert\Delta\mathcal{I}^{m}_{\mathrm{KL_{QRS}}}\rvert$	0.5 ± 0.5	0.6 ± 0.6	0.3 ± 0.2	$5.9E{-}85$
$\Delta\mathcal{I}_{\mathrm{SNR}}$	-7.0 ± 69.3	-36.3 ± 79.7	-15.0 ± 31.6	$8.2E{-}16$
$\mathcal{I}_{\rho}$	0.2 ± 0.5	0.4 ± 0.5	-0.08 ± 0.5	$7.9E{-}69$
$\Delta\mathcal{I}_{\mathrm{Se}}$ [Hz]	0.11 ± 6.8	0.71 ± 5.11	-0.2 ± 7.1	0.09
$\Delta\mathcal{I}_{\mathrm{SI}}$ [Hz]	1.29 ± 8.0	1.9 ± 6.3	$-8E{-}5 \pm 7.5$	$2.0E{-}7$

(b) Confusion matrix

	Type	Prediction									
		Protocol A (EX = 72.0%)			Protocol B (EX = 82.3%)			Protocol C (EX = 85.4%)			
			IG	*HRG*	*SSG*	*IG*	*HRG*	*SSG*	*IG*	*HRG*	*SSG*
Percentage of events (%)	*IG*	50.8	25.6	23.6	59.7	21.3	19.0	62.8	18.5	18.7	
	HRG	12.3	67.4	20.3	15.9	66.4	17.7	14.8	64.3	20.9	
	SSG	4.2	7.1	88.7	2.0	3.5	94.6	3.5	1.9	94.6	
Included variables {V}		$\Delta\mathcal{I}_{\mathrm{RMS_{ST}}}$, $\mathcal{I}_{\mathrm{HR_3}}$, $\lvert\Delta\mathcal{I}^{e}_{\mathrm{KL_{ST-T}}}\rvert$, $\lvert\Delta\mathcal{I}_{\mathrm{HR}}\rvert$, $\mathcal{I}_{\rho}$, $\lvert\Delta\mathcal{I}^{m}_{\mathrm{KL_{ST-T}}}\rvert$, $\Delta\mathcal{I}_{\mathrm{SNR}}$, $\Delta\mathcal{I}_{\mathrm{ST}}$, $\lvert\Delta\mathcal{I}^{m}_{\mathrm{KL_{QRS}}}\rvert$, $\lvert\Delta\mathcal{I}^{e}_{\mathrm{KL_{QRS}}}\rvert$, $\lvert\mathcal{I}_{\mathrm{ST}}\rvert$ and $\lvert\Delta\mathcal{I}_{\mathrm{RMS_{ST}}}\rvert$			$\Delta\mathcal{I}_{\mathrm{RMS_{ST}}}$, $\lvert\Delta\mathcal{I}_{\mathrm{HR}}\rvert$, $\lvert\Delta\mathcal{I}^{e}_{\mathrm{KL_{ST-T}}}\rvert$, $\mathcal{I}_{\rho}$, $\lvert\Delta\mathcal{I}^{m}_{\mathrm{KL_{ST-T}}}\rvert$, $\mathcal{I}_{\mathrm{HR_3}}$, $\Delta\mathcal{I}_{\mathrm{SNR}}$, $\Delta\mathcal{I}_{\mathrm{ST}}$, $\mathcal{I}_{\mathrm{Se}}$ and $\mathcal{I}_{\mathrm{SI}}$			$\Delta\mathcal{I}_{\mathrm{RMS_{ST}}}$, $\lvert\Delta\mathcal{I}^{e}_{\mathrm{KL_{ST-T}}}\rvert$, $\lvert\Delta\mathcal{I}_{\mathrm{HR}}\rvert$, $\lvert\Delta\mathcal{I}^{m}_{\mathrm{KL_{QRS}}}\rvert$, $\mathcal{I}_{\mathrm{HR_3}}$, $\Delta\mathcal{I}_{\mathrm{SNR}}$, $\mathcal{I}_{\rho}$ and $\Delta\mathcal{I}_{\mathrm{ST}}$		

Five variables were calculated to assess the classification performance: sensitivity (SE), specificity (SP), positive predictivity value (+PV), negative predictivity value (−PV) and exactness (EX). SE, +PV, SP and −PV when clustering a group "1" from another group "2", are defined as follows:

$$SE = \frac{TP}{TP + FN} \qquad +PV = \frac{TP/N_1}{TP/N_1 + FP/N_2}$$
$$SP = \frac{TN}{TN + FP} \qquad -PV = \frac{TN/N_2}{TN/N_2 + FN/N_1}$$

while *EX*, also called accuracy, is defined as:

$$EX = \frac{TP + TN}{N_1 + N_2}$$

where *TP* represents the true positives, *FN* the false negatives, *FP* the false positives, *TN* the true negatives and N_1 and N_2 are the number of elements belonging to the group "1" and "2" respectively. The normalization factors (N_1 and N_2) when estimating the +PV are due to the imbalance of the number of elements in each group involved in the discriminant analysis (see Table 1(b)).

3. Results

3.1. Classification between IG, HRG and SSG

For the ANOVA classification, variables related to the T wave delineation such as $\Delta\mathcal{I}_{\mathrm{QT}}$, $\Delta\mathcal{I}_{\mathrm{TA}}$, $\Delta\mathcal{I}_{T_w}$ and $\Delta\mathcal{I}_{T_{pe}}$, have not been included because body position changes linked to high noisy beats make T wave delineation problematic. In Table 2(a), means and standard deviations of each index for each type of episode are shown for protocol B.

Multivariate discriminant analysis results for classifying the three groups (*IG*, *HRG* and *SSG*) are presented in terms of the confusion matrix in Table 2(b) for the three protocols A, B and C. The selected set of variables {V} ordered by significance of the

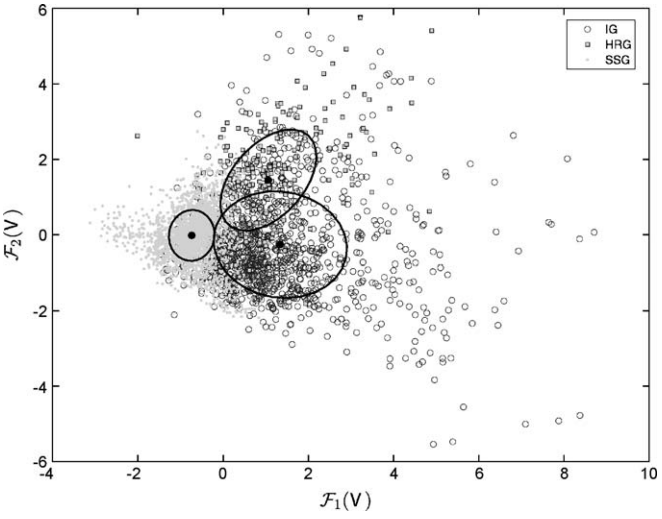

Fig. 4. Group dispersion diagrams for the discriminant functions $\mathcal{F}_1$(V) and $\mathcal{F}_2$(V), obtained using the set of indices giving the best performance for protocol B. The standard deviation and the mean value of each group distribution are also shown.

Table 3
Summary of the classification performance in terms of sensitivity (SE), specificity (SP) and exactness (EX) between transient events *TG* (ischemic plus heart rate related episodes) and sudden ST shifts (*SSG*) for the annotation protocols A, B and C. The variables included for the classification for each protocol are also shown.

Events	Protocol A (EX = 82.7%)		Protocol B (EX = 90.5%)		Protocol C (EX = 93.0%)	
	SE (%)	SP (%)	SE (%)	SP (%)	SE (%)	SP (%)
TG vs. *SSG*	71.6	93.3	76.8	98.3	78.3	99.0
Included variables {V}	$\Delta\mathcal{I}_{\mathrm{RMS_{ST}}}$, $\lvert\Delta\mathcal{I}^{e}_{\mathrm{KL_{ST-T}}}\rvert$, $\lvert\Delta\mathcal{I}_{\mathrm{HR}}\rvert$, $\mathcal{I}_{\rho}$, $\lvert\Delta\mathcal{I}^{m}_{\mathrm{KL_{ST-T}}}\rvert$, $\mathcal{I}_{\mathrm{HR_3}}$, $\Delta\mathcal{I}_{\mathrm{SNR}}$, $\Delta\mathcal{I}_{\mathrm{SI}}$ and $\Delta\mathcal{I}_{\mathrm{Se}}$		$\Delta\mathcal{I}_{\mathrm{RMS_{ST}}}$, $\lvert\Delta\mathcal{I}^{e}_{\mathrm{KL_{ST-T}}}\rvert$, $\lvert\Delta\mathcal{I}_{\mathrm{HR}}\rvert$, $\mathcal{I}_{\rho}$, $\lvert\Delta\mathcal{I}^{m}_{\mathrm{KL_{ST-T}}}\rvert$, $\mathcal{I}_{\mathrm{HR_3}}$, $\Delta\mathcal{I}_{\mathrm{SNR}}$, $\Delta\mathcal{I}_{\mathrm{SI}}$ and $\Delta\mathcal{I}_{\mathrm{Se}}$		$\Delta\mathcal{I}_{\mathrm{RMS_{ST}}}$, $\lvert\Delta\mathcal{I}^{e}_{\mathrm{KL_{ST-T}}}\rvert$, $\lvert\Delta\mathcal{I}_{\mathrm{HR}}\rvert$, $\mathcal{I}_{\rho}$, $\lvert\Delta\mathcal{I}^{m}_{\mathrm{KL_{ST-T}}}\rvert$, $\mathcal{I}_{\mathrm{HR_3}}$, $\Delta\mathcal{I}_{\mathrm{SNR}}$, $\Delta\mathcal{I}_{\mathrm{SI}}$ and $\Delta\mathcal{I}_{\mathrm{Se}}$	

classification for each annotation protocol is also included below the confusion matrix.

The group dispersion diagram obtained with the two discriminant functions, $\mathcal{F}_1$(V) and $\mathcal{F}_2$(V), for protocol B, is shown in Fig. 4.

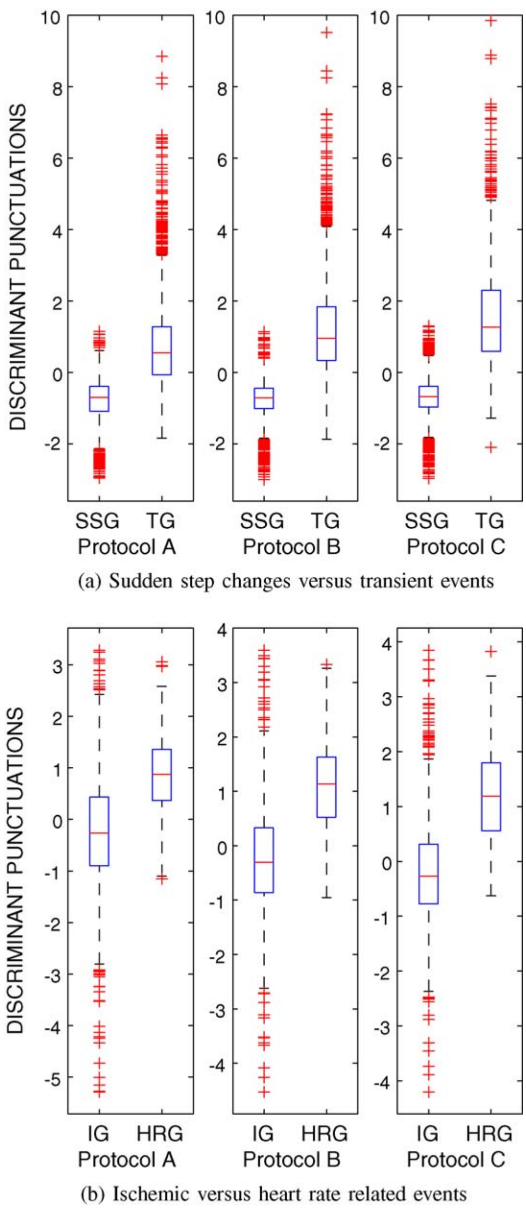

Fig. 5. (a) Discriminant punctuation for classifying between the transient group (*TG*) and the sudden step group (*SSG*) for the three protocols. (b) Discriminant punctuation for classifying between the ischemic (*IG*) and the heart rate related (*HRG*) group for the three protocols.

3.2. Classification between different ST level patterns: TG and SSG

As regards distinguishing between different ST signatures, the *TG* and the *SSG*, results are shown in Table 3 in terms of SE, SP and EX. The most significant variables selected by the classification analysis for each protocol are also shown.

In order to represent the discriminant punctuation classifying the *TG* and *SSG* for the three protocols, box plots have been used (see Fig. 5(a)). Each box plot represents the 25–75th percentile and the line within the box denotes the mean.

3.3. Discrimination between the ischemic group (IG) and the heart rate related group (HRG)

For classifying *IG* and *HRG* events, we have first used all the variables except the T wave related indices, reaching an accuracy of 77.2% for protocol B. The selected set of variables for protocol B used in the classification analysis is: $\mathcal{I}_{\mathrm{HR_3}}$, $\lvert\Delta\mathcal{I}^{e}_{\mathrm{KL_{ST-T}}}\rvert$, $\Delta\mathcal{I}_{\mathrm{ST}}$, $\lvert\Delta\mathcal{I}_{\mathrm{HR}}\rvert$, $\Delta\mathcal{I}_{\mathrm{RMS}}$, $\mathcal{I}_{\rho}$, $\lvert\Delta\mathcal{I}^{m}_{\mathrm{KL_{QRS}}}\rvert$, $\lvert\Delta\mathcal{I}^{e}_{\mathrm{KL_{QRS}}}\rvert$ and $\Delta\mathcal{I}_{\mathrm{SNR}}$.

In order to improve the discrimination performance, we have added the T wave related variables and included changes between the three different intervals I_1, I_2 and I_3.

The mean and the standard deviation of several variables evaluated in the discriminant analysis for the two different groups (*IG* and *HRG*) are presented in Table 4(a). The performance analysis and the *p*-value of the discrimination between the groups have also been evaluated for each variable individually.

Table 4(b) shows the classification performance for protocol B, in terms of SE, SP, +PV and −PV, obtained when adding new T wave related variables in the stepwise approach and also a summary of the performance and the selected set of variables for protocols A and C.

The discriminant punctuation between *IG* and *HRG* calculated analogously to the the discrimination between *TG* and *SSG* is shown in Fig. 5(b).

3.4. Classification between IG and NIG

The performance analysis when distinguishing between *IG* and *NIG* (*HRE*, *BPCE* and *CCE*) reaches an exactness of 87.5% for protocol B. A summary of the classification performance is shown in Table 5.

Classification of episodes on each recording (patient) has been calculated using leave-one-out over recordings. The percentages of patients whose sensitivity, specificity and exactness are within the ranges: less than 50%, from 50% to 60%, from 60% to 70% and so on until more than 90% are shown in Fig. 6.

4. Discussion

4.1. Classification between IG, HRG and SSG

In the first part of this work we have approached the task of classifying the three different types of ST events, *IE*, *HRE* and *SSE*,

Table 4
(a) Summary of the mean and the standard deviation (mean ± std) of different indices variations used for the classification analysis of the annotated ischemic (*IG*) and heart rate related episodes (*HRG*). The *p*-value of those indices is also shown. (b) shows the improvement in classification performance between *IG* and *HRG* episodes in terms of SE, SP, +PV, −PV and EX, in each step of the method for protocol B. A summary of the performance together with the selected set of variables for protocols A and C is also shown.

(a) Statistical description of each index

Variables	*IG*	*HRG*	*p*-Value
$\Delta\mathcal{I}_{\mathrm{RMS}_{ST13}}$ [μV]	37.4 ± 24.8	22.8 ± 16.2	$4E{-}09$
$\Delta\mathcal{I}_{\mathrm{ST}_{13}}$ [μV]	-69.87 ± 148.2	-26.54 ± 107.6	0.003
$\lvert\Delta\mathcal{I}_{\mathrm{ST}_{13}}\rvert$ [μV]	140.28 ± 84.53	98.8 ± 49.5	$6E{-}07$
$\lvert\Delta\mathcal{I}_{\mathrm{HR}_{12}}\rvert$ [bpm]	3.8 ± 4	8.4 ± 7.1	$2E{-}21$
$\lvert\Delta\mathcal{I}_{\mathrm{HR}_{13}}\rvert$ [bpm]	10.07 ± 9.4	19.16 ± 11.14	$6E{-}19$
$\mathcal{I}_{\mathrm{HR}_3}$ [bpm]	85.6 ± 19.9	103.6 ± 20.7	$2E{-}17$
$\Delta\mathcal{I}_{\mathrm{QT}_{13}}$ [ms]	-5.2 ± 28.2	-30.6 ± 34	$1.2E{-}16$
$\Delta\mathcal{I}_{\mathrm{QT}_{23}}$ [ms]	-3.8 ± 24.9	2.5 ± 30	$8E{-}16$
$\Delta\mathcal{I}_{Tw_{13}}$ [ms]	-18.1 ± 27.1	-32.9 ± 40.3	$1E{-}06$
$\Delta\mathcal{I}_{Tpe13}$ [ms]	-5.8 ± 14.2	-12.9 ± 22.2	$1E{-}05$
$\lvert\Delta\mathcal{I}^{e}_{\mathrm{KL}_{\mathrm{QRS}_{12}}}\rvert$	0.03 ± 0.03	0.02 ± 0.02	0.008
$\lvert\Delta\mathcal{I}^{e}_{\mathrm{KL}_{\mathrm{ST-T}_{13}}}\rvert$	0.03 ± 0.03	0.02 ± 0.02	$6E{-}08$
$\lvert\Delta\mathcal{I}^{m}_{\mathrm{KL}_{\mathrm{ST-T}_{12}}}\rvert$	0.04 ± 0.3	-0.06 ± 0.3	0.046
$\Delta\mathcal{I}_{\mathrm{SI}_{23}}$ [Hz]	0.35 ± 5.87	1.75 ± 5.19	0.02
$\Delta\mathcal{I}_{\mathrm{Se}_{23}}$ [Hz]	-0.41 ± 5.06	0.87 ± 4.12	0.01
$\mathcal{I}_{\rho}$	-0.16 ± 0.5	0.36 ± 0.5	$1E{-}04$
$\Delta\mathcal{I}_{\mathrm{SNR}_{13}}$	-4.2 ± 70.4	-39.7 ± 84.4	$2.3E{-}06$
$\Delta\mathcal{I}_{\mathrm{TA}_{13}}$ [μV]	-37.2 ± 271.2	-116.8 ± 201.9	0.003

(b) Step-wise classification

	Variables (ordered by classification relevance)	SE	SP	+PV	−PV	EX
P	$\lvert\Delta\mathcal{I}_{\mathrm{HR}_{12}}\rvert$	78.7	54.5	63.4	71.9	75.0
R	$\lvert\Delta\mathcal{I}_{\mathrm{HR}_{12}}\rvert$, $\Delta\mathcal{I}_{\mathrm{QT}_{23}}$	80.5	67.0	70.9	77.4	78.4
O	$\lvert\Delta\mathcal{I}_{\mathrm{HR}_{12}}\rvert$, $\Delta\mathcal{I}_{\mathrm{QT}_{23}}$, $\lvert\Delta\mathcal{I}_{\mathrm{ST}_{13}}\rvert$	81.0	68.8	72.2	78.3	79.1
T	$\lvert\Delta\mathcal{I}_{\mathrm{HR}_{12}}\rvert$, $\Delta\mathcal{I}_{\mathrm{QT}_{23}}$, $\lvert\Delta\mathcal{I}_{\mathrm{ST}_{13}}\rvert$, $\Delta\mathcal{I}_{\mathrm{ST}_{13}}$	80.3	79.5	79.6	80.2	80.2
O	$\lvert\Delta\mathcal{I}_{\mathrm{HR}_{12}}\rvert$, $\Delta\mathcal{I}_{\mathrm{QT}_{23}}$, $\lvert\Delta\mathcal{I}_{\mathrm{ST}_{13}}\rvert$, $\Delta\mathcal{I}_{\mathrm{ST}_{13}}$, $\mathcal{I}_{\mathrm{HR}_3}$	83.5	76.8	78.2	82.3	82.5
C	$\lvert\Delta\mathcal{I}_{\mathrm{HR}_{12}}\rvert$, $\Delta\mathcal{I}_{\mathrm{QT}_{23}}$, $\lvert\Delta\mathcal{I}_{\mathrm{ST}_{13}}\rvert$, $\Delta\mathcal{I}_{\mathrm{ST}_{13}}$, $\mathcal{I}_{\mathrm{HR}_3}$, $\lvert\Delta\mathcal{I}^{e}_{\mathrm{KL}_{\mathrm{ST-T}_{13}}}\rvert$	82.7	82.1	82.2	82.6	82.6
O	$\lvert\Delta\mathcal{I}_{\mathrm{HR}_{12}}\rvert$, $\Delta\mathcal{I}_{\mathrm{QT}_{23}}$, $\lvert\Delta\mathcal{I}_{\mathrm{ST}_{13}}\rvert$, $\Delta\mathcal{I}_{\mathrm{ST}_{13}}$, $\mathcal{I}_{\mathrm{HR}_3}$, $\lvert\Delta\mathcal{I}^{e}_{\mathrm{KL}_{\mathrm{ST-T}_{13}}}\rvert$, $\lvert\Delta\mathcal{I}_{\mathrm{HR}_{13}}\rvert$	83.8	81.3	81.7	83.4	83.4
L	$\lvert\Delta\mathcal{I}_{\mathrm{HR}_{12}}\rvert$, $\Delta\mathcal{I}_{\mathrm{QT}_{23}}$, $\lvert\Delta\mathcal{I}_{\mathrm{ST}_{13}}\rvert$, $\Delta\mathcal{I}_{\mathrm{ST}_{13}}$, $\mathcal{I}_{\mathrm{HR}_3}$, $\lvert\Delta\mathcal{I}^{e}_{\mathrm{KL}_{\mathrm{ST-T}_{13}}}\rvert$, $\lvert\Delta\mathcal{I}_{\mathrm{HR}_{13}}\rvert$, $\lvert\Delta\mathcal{I}^{e}_{\mathrm{KL}_{\mathrm{QRS}_{12}}}\rvert$	84.0	85.7	85.5	84.3	84.3
B	$\lvert\Delta\mathcal{I}_{\mathrm{HR}_{12}}\rvert$, $\Delta\mathcal{I}_{\mathrm{QT}_{23}}$, $\lvert\Delta\mathcal{I}_{\mathrm{ST}_{13}}\rvert$, $\Delta\mathcal{I}_{\mathrm{ST}_{13}}$, $\mathcal{I}_{\mathrm{HR}_3}$, $\lvert\Delta\mathcal{I}^{e}_{\mathrm{KL}_{\mathrm{ST-T}_{13}}}\rvert$, $\lvert\Delta\mathcal{I}_{\mathrm{HR}_{13}}\rvert$, $\lvert\Delta\mathcal{I}^{e}_{\mathrm{KL}_{\mathrm{QRS}_{12}}}\rvert$ and $\Delta\mathcal{I}^{m}_{\mathrm{KL}_{\mathrm{QRS}_{23}}}$	84.5	86.6	86.3	84.8	84.8
A	$\mathcal{I}_{\mathrm{HR}_3}$, $\Delta\mathcal{I}_{\mathrm{ST}_{13}}$, $\lvert\Delta\mathcal{I}^{e}_{\mathrm{KL}_{\mathrm{ST-T}_{13}}}\rvert$, $\lvert\Delta\mathcal{I}_{\mathrm{HR}_{13}}\rvert$, $\Delta\mathcal{I}_{\mathrm{RMS}_{ST23}}$, $\Delta\mathcal{I}_{Tpe12}$, $\lvert\Delta\mathcal{I}^{e}_{\mathrm{KL}_{\mathrm{QRS}_{12}}}\rvert$, $\lvert\Delta\mathcal{I}^{m}_{\mathrm{KL}_{\mathrm{QRS}_{13}}}\rvert$, $\Delta\mathcal{I}_{\mathrm{SNR}_{12}}$, $\lvert\Delta\mathcal{I}_{\mathrm{HR}_{12}}\rvert$, $\lvert\Delta\mathcal{I}^{e}_{\mathrm{KL}_{\mathrm{ST-T}_{12}}}\rvert$ and $\lvert\Delta\mathcal{I}^{m}_{\mathrm{KL}_{\mathrm{ST-T}_{12}}}\rvert$	76.0	76.5	76.4	76.1	76.1
C	$\lvert\Delta\mathcal{I}_{\mathrm{HR}_{12}}\rvert$, $\Delta\mathcal{I}_{\mathrm{HR}_{13}}$, $\Delta\mathcal{I}_{\mathrm{ST}_{13}}$, $\Delta\mathcal{I}_{\mathrm{RMS}_{ST23}}$, $\Delta\mathcal{I}_{\mathrm{SI}_{23}}$, $\mathcal{I}_{\mathrm{HR}_3}$ and $\Delta\mathcal{I}_{\mathrm{SNR}_{12}}$	86.5	81.5	82.4	85.8	86.0

Table 5
Summary of the classification performance in terms of sensitivity (SE) and specificity (SP) between the ischemic group *IG* and the non-ischemic group *NIG* for the annotation protocols A, B and C. The variables included for the classification for each protocol are also shown.

Events	Protocol A (EX = 79.0%)		Protocol B (EX = 87.5%)		Protocol C (EX = 91.0%)	
	SE(%)	SP(%)	SE(%)	SP(%)	SE(%)	SP(%)
IG vs. NIG	65.0	87.7	74.2	93.2	77.7	95.6
Included variables {V}	$\Delta\mathcal{I}_{\mathrm{RMS}_{\mathrm{ST}}}$, $\lvert\Delta\mathcal{I}^{e}_{\mathrm{KL}_{\mathrm{ST-T}}}\rvert$, $\Delta\mathcal{I}_{\mathrm{SNR}}$, $\mathcal{I}_{\rho}$, $\Delta\mathcal{I}_{\mathrm{ST}}$, $\lvert\Delta\mathcal{I}^{m}_{\mathrm{KL}_{\mathrm{ST-T}}}\rvert$, $\Delta\mathcal{I}_{\mathrm{Se}}$ and $\Delta\mathcal{I}_{\mathrm{SI}}$		$\Delta\mathcal{I}_{\mathrm{RMS}_{\mathrm{ST}}}$, $\lvert\Delta\mathcal{I}^{e}_{\mathrm{KL}_{\mathrm{ST-T}}}\rvert$, $\lvert\Delta\mathcal{I}^{m}_{\mathrm{KL}_{\mathrm{ST-T}}}\rvert$, $\Delta\mathcal{I}_{\mathrm{SNR}}$, $\mathcal{I}_{\rho}$, $\Delta\mathcal{I}_{\mathrm{SI}}$, $\Delta\mathcal{I}_{\mathrm{Se}}$ and $\lvert\Delta\mathcal{I}_{\mathrm{HR}}\rvert$		$\Delta\mathcal{I}_{\mathrm{RMS}_{\mathrm{ST}}}$, $\lvert\Delta\mathcal{I}^{e}_{\mathrm{KL}_{\mathrm{ST-T}}}\rvert$, $\lvert\Delta\mathcal{I}^{m}_{\mathrm{KL}_{\mathrm{ST-T}}}\rvert$, $\Delta\mathcal{I}_{\mathrm{SNR}}$, $\mathcal{I}_{\rho}$, $\Delta\mathcal{I}_{\mathrm{SI}}$ $\Delta\mathcal{I}_{\mathrm{Se}}$ and $\lvert\Delta\mathcal{I}_{\mathrm{HR}}\rvert$	

obtaining an accuracy of 82.3% and using a set of 11 indices for protocol B (see Table 2(b)). The ordered index set proposed as significant by the step wise approach is shown for each protocol. Note that the two most significant indices are $\Delta\mathcal{I}_{\mathrm{RMS}_{\mathrm{ST}}}$ followed by $|\Delta\mathcal{I}_{\mathrm{HR}}|$. The first shows a first attempt to classify the two different patterns of the ST level, the transient *TG* and the sudden step group *SSG*, while the second shows greater differences within the *TG*, between *IE* and *HRE*.

If we analyse each index individually (see Table 2(a)), $\Delta\mathcal{I}_{\mathrm{RMS}_{\mathrm{ST}}}$ associated to changes in energy of the ST segment, is higher in the *IG* (38.7 μV) than in the *HRG* (24.9 μV) and hardly changes in the *SSG* (−0.2 μV). These results agree with indices $\Delta\mathcal{I}_{\mathrm{ST}}$ and $|\Delta\mathcal{I}_{\mathrm{ST}}|$, which show greater values in the *TG* (more in the *IG* than in the *HRG*) than in the *SSG* group, where the ST level change is abrupt and with low amplitude.

Heart rate related indices show higher increments during *HRE* ($|\Delta\mathcal{I}_{\mathrm{HR}}| \simeq 22.1$ bpm) in comparison with *IE* ($\simeq 12.1$ bpm) and *SSE* ($\simeq 6.5$ bpm). The heart rate value at the extremum is also higher in mean during *HRE* ($\simeq 110.2$ bpm) than during *IE* ($\simeq 90.5$ bpm) and much more than in *SSE* ($\simeq 82.6$ bpm).

The KL-based indices, associated to changes in the QRS and ST–T complexes and mostly used to detect body position changes in the ECG [15], show higher differences between the *TG* and the *SSG* than within the *TG* (*IG* and *HRG*).

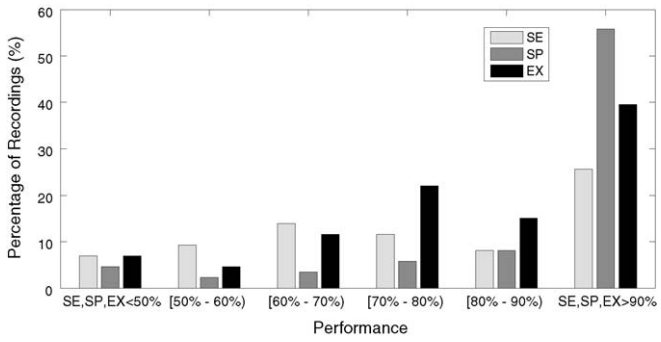

Fig. 6. Percentage of recordings whose sensitivity, specificity and exactness when detecting ischemia are within different ranges.

The early and the late QRS slopes show differences between the transient ($\Delta\mathcal{I}_{\mathrm{SI}} \simeq 1.56$ Hz) and the sudden step group ($\Delta\mathcal{I}_{\mathrm{SI}} \simeq 0.06$ Hz).

Index $\mathcal{I}_{\rho}$, associated to the correlation between the heart rate and the RMS of the ST segment is higher in mean in *HRG* events ($\simeq 0.4$) than in *IG* events ($\simeq 0.2$), showing that an increase of heart rate in *IE* could be secondary to the oxygen demand-supply imbalance while in *HRE*, the ST segment change is directly the result of T wave incursion into the ST segment because of the high heart rate. *SSG* events hardly show correlation in mean ($\simeq -0.08$).

In terms of protocols, protocol C, with the least number of transient events and the most restrictive, achieves the highest accuracy when classifying, followed by protocols B and A, the least restrictive. This is in accordance with the fact that protocol C retains only the very evident episodes.

4.2. Classification between different ST level patterns: TG and SSG

The very different origins and patterns of the ST level in the *TG* and the *SSG* result in the accuracy of distinguishing between these two groups increasing up to 90.5% for protocol B (see Table 3). The sensitivity when classifying the *TG* is 77% and 98% for the *SSG*.

Most variables included in the classification analysis rely on changes in the ST segment, $\Delta\mathcal{I}_{\mathrm{RMS_{ST}}}$, associated to changes in the area defined by the ST segment, being the most significant index, followed by $|\Delta\mathcal{I}^{e}_{\mathrm{KL_{ST-T}}}|$. This agrees with the fact that they have different ST level patterns.

KL-based indices of the ST–T and QRS are suggested in the literature as markers for the detection of body position changes [15] that are associated to sudden step ST changes, agreeing with our results that propose $|\Delta\mathcal{I}^{e}_{\mathrm{KL_{ST-T}}}|$ as a significant parameter in the discrimination. This index accounts for the complete repolarization feature, adding which could be missed by just looking at the ST segment exclusively.

ST level is also a crucial parameter for classification. Calculation of the deviation of the ST in mean for *TG* ($\simeq 130$ μV) is higher than in the *SSG* ($\simeq 48$ μV).

Information about heart rate is also included in the discriminant function. $|\Delta\mathcal{I}_{\mathrm{HR}}|$ shows greater changes in mean of heart rate during *TG* ($\simeq 12$ bpm) in comparison to *SSG* ($\simeq 2$ bpm).

4.3. Discrimination between the ischemic group (IG) and the heart rate related group (HRG)

A first attempt in distinguishing between *IE* and *HRE* without using T wave related indices achieved an accuracy of 77.2% for protocol B. However, the accuracy increases up to 84.8% when we add those indices related to the repolarization dispersion as described in Section 2.3.1 (see Table 4(b)).

Note that the variables with lower *p*-values are those related to heart rate and QT interval and thus the first ones included in the step wise approach are $|\Delta\mathcal{I}_{\mathrm{HR}_{12}}|$ and $\Delta\mathcal{I}_{\mathrm{QT}_{23}}$ (see Table 4).

HRE are mostly associated to more remarkable changes in heart rate than *IE* and in order to group these episodes the first variable included in the classification analysis is $|\Delta\mathcal{I}_{\mathrm{HR}_{12}}|$ ($\simeq 3.8$ bpm in mean for *IG* and $\simeq 8.4$ bpm for *HRG*). However, heart rate acceleration is also a key factor to induce ischemia in patients with coronary occlusion and therefore other indices in addition to the heart rate change related to changes in the *ST* segment are needed to avoid overlapping with the *HRG*. Regarding the *IG*, in [24] it is claimed that much larger number of the records of the LTST DB contain demand ischemic episodes, related to heart rate. However, episodes in the database are not clinically classified as demand or supply episodes. Besides, care should be taken in the sense that not all episodes in *HRG* are associated with an increase in heart rate. In about 10% of the episodes, heart rate is oscillating or even decreasing.

QT interval changes are typically adapted to changes in the RR interval, therefore the QT interval is hardly shortened in *IE* ($\simeq 4$ ms) while in *HRE* it is reduced by about 28 ms.

Alterations in the late steepest slope has been proposed as an index to quantify ECG changes in supply ischemia, with the result that QRS slopes were considerably less steep during prolonged ($\simeq 4$ min) artery occlusion [22]. However, in short term ($\simeq 1$ min) angioplasty episodes, discrepant slope variations were found [25]. Our results show no systematic changes and agrees mostly with [25].

A greater shortening in the T width, in mean, is observed in *HRE* ($\simeq -32$ ms) while in *IE* it is lower ($\simeq -18$ ms). A similar behaviour is observed in $\Delta\mathcal{I}_{T_{pe}}$ where the shortening is greater in *HRE*. Both indices are closely related to heart rate with the difference that T_w interval adapts slower to heart rate changes than T_{pe} interval [26].

In general, transmural or epicardial ischemia is reflected in ST elevation while sub-endocardial ischemia shows ST depression [3]. Our results (Table 4(a)) show depression in the ST level function during *IE* ($\backsim -70$ μV in mean) and agrees with [3] due to the fact that most of ischemic events in Holter recordings are sub-endocardial. The absolute deviation of the ST level is higher in *IE* ($\backsim 144$ μV in mean) than in *HRE* ($\backsim 93$ μV) as expected.

The amplitude of the T wave is reduced during both types of episodes, being lower during *HRE* in comparison to *IE*. The depression of the T wave agrees with [27], which states that epicardial ischemia increases the peak T amplitude while endocardial ischemia produces a size-dependent reduction in T amplitude. As we commented above most of the *IE* in Holter recordings are sub-endocardial.

Finally, note that in [7] it is also presented a discrimination between *IG* and *HRG*, reaching a sensitivity of 77.9% and a specificity of 73.9%. Without including T wave related variables, we obtained similar results. In this work, we added T wave related indices and achieved an increase up to 84.5% in sensitivity and up 86.6% in the specificity.

4.4. Classification between IG and NIG

When the classification target is ischemia, we observe that the two first variables that best distinguish between *IG* and *NIG* are those related to the ST segment: $\Delta\mathcal{I}_{\mathrm{RMS_{ST}}}$ and $|\mathcal{I}^{e}_{\mathrm{KL_{ST-T}}}|$. Note that these indices are also the most significant when distinguishing between different ST segment patterns (*TG* and *SSG*). The reason is that the *IG* has a much higher change in the RMS of the ST segment and also in the ST–T complex than *TG* and *SSG* (see Table 2(a)).

In relation with the Physionet/Computers in Cardiology Challenge, our results are comparable with [9] (EX = 90.7% in

[9] and EX = 87.5% with our method), being the ST level change a very substantial parameter for distinguishing between *IG* and *NIG*. However, [9] uses indices such as changes in the ST level manually corrected by experts while our method is fully automated.

Performance on recordings rather than on episodes, is shown in Fig. 6. About 30% of the patients have a sensitivity of more than 90% when the target is classifying *IE*, more than 50% have a specificity of 90% and 40% have an exactness of more than 90%. This means that most of the patients have more than 90% of the *NIE* correctly classified. On the other way round, less than 10% of the patients have a sensitivity, specificity and exactness less than 50% when classifying *IE*. We can conclude that this method minimizes the false positive classification and less than 10% of the patients have less of the 50% of *IE* correctly classified.

4.5. General remarks

An important limitation of this study is that although the expert annotations are used as gold standard, classification of a particular episode can be driven by a previous knowledge about the patient rather than physiological evidences. Also, the usage of different lead configurations in this database adds difficulties when classifying.

In addition to use the magnitude of the feature change to account for the dynamic effects of ST episodes, we have also considered to use the percentage change. However, this strategy was not as significant as the one related to the magnitude of the change when inserted in the discriminant analysis.

Due to the fact that some indices have leptokurtic distributions, a logarithmic transformation has also been tested. However, it has been discarded as no improvement was reached. This is in concordance with some studies that show that linear discriminant analysis is relatively robust even when there are modest violations of the assumptions of homogeneity of variances and normal distributions of indices [23].

In linear discriminant analysis, the covariance matrix of each of the classes is assumed to be identical. Quadratic discriminant analysis is a more general classifier where each class has a different covariance matrix. The usage of quadratic discriminant analysis has not improved the performance (about $\pm 0.5\%$ in exactness). Besides, the obtained performance in test set is similar to the one obtained in the training set. These results suggest that no improvement could be reached in linear classification and non-linear statistical techniques such as artificial neural networks and support vector machines could be explored as alternative classifiers. Non-linear indices to differentiate normal states from ischemic ones such as shifts in the Shannon's entropy could also be studied [28].

5. Conclusions

In this work we have used various indices to distinguish between different ST level change events, our target being to distinguish ischemia from artifactual events such as heart rate related episodes and sudden step changes annotated by experts in the LTST DB.

When discriminating between the three types of events (Task 1), the very pronounced differences between the transient episodes (*IE* and *HRE*) and the sudden step ST events, together with the differences in the number of episodes between groups, cause the step wise classification approach to focus first on classifying sudden step ST changes. The most significant variable of the discrimination function is related with changes in energy of the ST segment, showing a first classification between transient and sudden step changes. The second input variable is related to heart rate and attempts to discriminate between *IG* and *HRG*.

The results notably improve when trying to distinguish between the two very different ST level patterns: transient and sudden step (Task 2). As expected, the first included indices are $\Delta\mathcal{I}_{\mathrm{RMS}_{\mathrm{ST}}}$ and $|\mathcal{I}^{e}_{\mathrm{KL}_{\mathrm{ST-T}}}|$ related to changes in energy of the ST segment and the ST–T complex respectively.

For ischemia detectors based on changes in the ST segment, discrimination between *IE* and *HRE* (Task 3), both of which have very similar patterns in the ST level function, could prove to be a very useful tool for automatic screening of Holter episodes. The results show that further information such as heart rate indices, the QT interval or KL-based indices from both repolarization and depolarization, help in discriminating between them, allowing the sensitivity/specificity to increase to 84.5%/86.6%.

In order to diagnose pathological problems, we have attempted to discriminate between ischemic and non-ischemic events (Task 4). In this case, we achieved an accuracy of 87.5%.

List of acronyms

LTST DB	Long-Term ST Database
IE	ischemic episodes
HRE	heart rate episodes
BPCE	body position change episodes
CCE	conduction change episodes
TE	transient episodes
SSE	sudden step episodes
NIE	non-ischemic events
IG	ischemic group
HRG	heart rate group
TG	transient group
SSG	sudden step group
NIG	non-ischemic group
KLT	Karhunen–Loève Transform
T_w	T wave width
T_{pe}	T wave peak to T end interval

References

[1] J.E. Deanfield, M. Shea, M. Kensett, P. Horlock, R.A. Wilson, C.M. deLandsheere, A.P. Selwyn, Silent myocardial ischaemia due to mental stress, Lancet 2 (1984) 1001–1005.
[2] T.C. Andrews, T. Fenton, N. Toyosaki, S.P. Glasser, P.M. Young, G. MacCallum, R.S. Gibson, T.L. Shook, P.H. Stone, Subsets of ambulatory myocardial ischemia based on heart rate activity. circadian distribution and response to anti-ischemic medication, Circulation 88 (1993) 92–100.
[3] A. Bayés de Luna, Clinical Electrocardiography: A Textbook, Futura Publishing Company, Armonk, NY, 1998.
[4] J. García, L. Sörnmo, S. Olmos, P. Laguna, Automatic detection of ST–T complex changes on the ECG using filtered RMS difference series: application to ambulatory ischemia monitoring, IEEE Trans. Biomed. Eng. 47 (9) (2000) 1195–1201.
[5] A. Smrdel, F. Jager, Automated detection of transient ST-segment episodes in 24 h electrocardiograms, Med. Biol. Eng. Comput. 42 (2004) 303–311.
[6] F. Jager, A. Taddei, G.B. Moody, M. Emdin, G. Antolič, R. Dorn, A. Smrdel, C. Marchesi, R.G. Mark, Long-Term ST database: a reference for the development and evaluation of automated ischaemia detectors and for the study of the dynamics of myocardial ischaemia, Med. Biol. Eng. Comput. 41 (2003) 172–182.
[7] J. Faganeli, F. Jager, Automatic distinguishing between ischemia and heart-rate related transient ST segment episodes in ambulatory ECG records, in: Computers in Cardiology, 2008.
[8] G.B. Moody, F. Jager, Distinguishing ischemic from non-ischemic ST changes: the Physionet/Computers in Cardiology Challenge, in: Computers in Cardiology, IEEE Computer Society Press, 2003, pp. 235–237.
[9] P. Langley, E.J. Bowers, J. Wild, M.J. Drinnan, J. Allen, A.J. Sims, N. Brown, A. Murray, An algorithm to distinguish ischaemic and non ischaemic ST changes in the Holter ECG, pp. 239–242, in: Computers in Cardiology, 2003.
[10] J.P. Martínez, P. Laguna, S. Olmos, O. Pahlm, J. Pettersson, L. Sörnmo, Assessment of QT-measurement accuracy using the 12-lead electrocardiogram derived from easi leads, J. Electrocardiol. 40 (2) (2007) 172–179.

[11] G.B. Moody, R.G. Mark, Development and evaluation of a 2-lead ECG analysis program, in: Computers in Cardiology, IEEE Comput. Soc. Press, Los Alamitos, 1982, pp. 39–44.
[12] C.R. Meyer, H.N. Keiser, Electrocardiogram baseline noise estimation and removal using cubic splines and state-space computation techniques, Comput. Biomed. Res. 10 (1977) 459–470.
[13] A. Mincholé, B. Skarp, F. Jager, P. Laguna, Evaluation of a root mean square based ischemia detector on the LTST database, in: XXXII Ann. Conf. Computers in Cardiology, Lyon, (2005), pp. 853–856.
[14] F. Badilini, W. Zareba, E.L. Titlebaum, A.J. Moss, Analysis of ST segment variability in Holter recordings, in: Noninvasive Electrocardiology: Clinical Aspects of Holter Monitoring. Frontiers in Cardiology, Saunders, London, UK, 1996, pp. 357–372.
[15] J. García, M. Astrom, J. Mendive, P. Laguna, L. Sörnmo, ECG-based detection of body position changes in ischemia monitoring, IEEE Trans. Biomed. Eng. 25 (6) (2003) 501–507.
[16] F. Jager, R.G. Mark, G.B. Moody, S. Divjak, Analysis of transient ST segment changes during ambulatorymonitoring using the Karhunen–Loeve transform, in: Computers in Cardiology, IEEE Comput. Soc. Press, 1992, pp. 691–694.
[17] P. Laguna, G.B. Moody, J. García, A. Goldberger, R.G. Mark, Analysis of the ST–T complex of the electrocardiogram using the Karhunen–Loéve transform: adaptive monitoring and alternans detection, Med. Biol. Eng. Comput. 37 (1999) 175–189.
[18] P. Arini, G.C. Beltran, E.R. Valverde, P. Laguna, T-wave width as an index for quantification of ventricular repolarization dispersion: evaluation in an isolated rabbit heart model, in: Biomedical Signal Processing and Control, vol. 3, Elsevier, 2008, pp. 67–77.
[19] J.P. Martínez, R. Almeida, S. Olmos, A.P. Rocha, P. Laguna, A wavelet-based ECG delineator: evaluation on standard databases, IEEE Trans. Biomed. Eng. 51 (4) (2004) 570–581.
[20] G.X. Yan, C. Antzelevitch, Cellular basis for the normal T wave and the electrocardiographic manifestations of the long-QT syndrome, Circulation 98 (1998) 1928–1936.
[21] E. Watanabe, I. Kodama, M. Ohono, H. Hishida, Electrocardiographic prediction of the development and site of acute myocardial infarction in patients with unstable angina, Int. J. Cardiol. (89) (2003) 231–237.
[22] E. Pueyo, L. Sörnmo, P. Laguna, QRS slopes for detection and characterization of myocardial ischemia, IEEE Trans. Biomed. Eng. 55 (2) (2008) 468–568.
[23] P.A. Lachenbruch, Discriminant Analysis, Hafner Press, 1975.
[24] A. Smrdel, F. Jager, Diurnal changes of heart rate and sympathovagal activity for temporal patterns of transient ischemic episodes in 24-hour electrocardiograms, EURASIP J. Adv. Signal Process. 2007 (2007) 10, Article ID 32386.
[25] G. Dory, A. Rosenthal, S. Fischman, Y. Denekamp, B.S. Lewis, H. Bitterman, Changes in the slope of the first major deflection of the ECG complex during acute coronary occlusion, Comput. Biol. Med. 35 (2005) 299–309.
[26] A. Mincholé, E. Pueyo, P. Laguna, Transmural differences in rate adaptation of repolarization duration quantified from ECG repolarization interval dynamics, Computers in Cardiology (2009).
[27] H. Ritsema van Eck, J. Kors, G. van Herpen, Effect of ischemic action potentials on T and U waves in the electrocardiogram, J. Electrocardiol. 40 (2007) S76.
[28] D. Lemire, C. Pharand, J.-C. Rajaonah, B. Dubé, A.-R. LeBlanc, Wavelet time entropy, T wave morphology and myocardial ischemia, IEEE Trans. Biomed. Eng. 47 (7) (2000) 967–970.